Methane efflux from an American bison herd

Paul C. Stoy[1,2,3]*, Adam A. Cook[3], John E. Dore[3,4], Natascha Kljun[5], William Kleindl[3], E. N. Jack Brookshire[3], Tobias Gerken[6]

[1]Department of Biological Systems Engineering, University of Wisconsin, Madison, WI, USA
[2]Department of Atmospheric and Oceanic Sciences, University of Wisconsin, Madison, WI, USA
[3]Department of Land Resources and Environmental Sciences, Montana State University, Bozeman, MT, USA
[4]Montana Institute on Ecosystems, Montana State University, Bozeman, MT, USA
[5]Centre for Environmental and Climate Research, Lund University, Lund, Sweden
[6]Department of Meteorology and Atmospheric Science, The Pennsylvania State University, University Park, PA, USA

Correspondence to: Paul C. Stoy (pcstoy@wisc.edu)

Abstract. American bison (*Bison bison* L.) have recovered from the brink of extinction over the past century. Bison reintroduction creates multiple environmental benefits, but impacts on greenhouse gas emissions are poorly understood. Bison are thought to have produced some 2 Tg year^{-1} of the estimated 9-15 Tg year^{-1} of pre-industrial enteric methane emissions, but few contemporary measurements have been made due to their mobile grazing habits and safety issues associated with direct measurements. Here, we measure methane and carbon dioxide fluxes from a bison herd on an enclosed pasture during daytime periods in winter using eddy covariance. Methane emissions from the study area were negligible in the absence of bison (mean ± standard deviation = −0.0009 ± 0.008 μmol m^{-2} s^{-1} μmol m^{-2} s^{-1}) and were significantly greater than zero, 0.048 ± 0.082 μmol m^{-2} s^{-1} with a positively skewed distribution, when bison were present. We coupled bison location estimates from automated camera images with two independent flux footprint models to calculate methane efflux on a per-animal basis, which varied from 55 μmol s^{-1} bison^{-1} to 62 μmol s^{-1} bison^{-1}. Per-animal methane efflux estimates were also sensitive to uncertanties in bison location, and sensitivity analyses suggest that a conservative uncertainty estimate is on the order of 22%. Combined with conservative uncertainty estimates of the eddy covariance measurements themselves, we arrive at methane flux estimates of 76 ± 21 g CH_4 bison^{-1} day^{-1} when using the Hsieh et al. (2000) model and 86 ± 24 g CH_4 bison^{-1} day^{-1} when using the Kljun et al. (2015) model, similar to eddy covariance measurements of methane efflux from a cattle feedlot during winter. Annual measurements are ultimately necessary to determine the full greenhouse gas burden of bison grazing systems. Our observations point to the need for direct comparisons of methane emissions from conventional and alternate grazing systems using eddy covariance and demonstrate the potential for using eddy covariance to measure methane efflux from non-domesticated animals.

1 Introduction

The American bison (*Bison bison* L.) was hunted to near extinction during European expansion across North America (Flores 1991, Isenberg 2000, Smits 1995). Fewer than 100 reproductive individuals existed on private ranches in the United States during the late 19th Century from an original population of 30 – 60 million (Hedrick, 2009). The current bison population of about 500,000 is due to the collective efforts of sovereign Indian tribes, government agencies, and private landowners (Gates et al., 2010; Sanderson et al., 2008; Zontek, 2007), all of whom have spurred a growing interest in bison reintroduction. The bison population is likely to further increase, increasing the incentive for researchers and land managers to understand the environmental impacts of their expansion.

The ecological role of bison has become better understood as populations have recovered (Allred et al., 2001; Hanson 1994; Knapp et al., 1999). Bison feed preferentially on grasses (Plumb and Dodd, 1993; Steuter and Hidinger, 1999) and enhance forb diversity as a result (Collins, 1998; Hartnett et al., 1996, Towne et al., 2005). They tend to graze in preferred meadows during winter and search broadly for the most energy-dense forages in summer (Fortin et al., 2003), often in areas which have recently burned (Allred et al., 1991; Coppedge and Shaw, 1998; Vinton et al., 1993). Bison also need not migrate to follow the 'green wave' of fresh vegetation during spring green-up like other ungulates; rather, their vigorous grazing tends to stimulate plant growth and create fresh, nutrient-rich foliage (Geremia et al., 2019). Combined, these observations suggest that bison select for forage quality rather than quantity which likely impacts their efflux of methane – which all ruminants emit – because ruminant methane emission is related to the cellulose and hemicellulose intake of their diet (Moe and Tyrrell, 1979) and feed quality (Hammond et al., 2016). It remains unclear how much methane results from the cellulose-rich grass-dominated diet of bison given their preference for fresh foliage and if management for bison may increase or diminish the greenhouse gas burden of ruminant-based agriculture.

Atmospheric methane concentrations have been rising at an accelerated rate since 2016 for reasons that remain unclear (Nisbet et al., 2019) and there is an urgent need to improve our understanding of its surface-atmosphere flux. Between 30 and 40 percent of current anthropogenic methane emissions are due to enteric fermentation in livestock (Kirschke et al., 2013) and the greenhouse gas burden of cattle alone is some 5 Pg of carbon dioxide equivalent per year (Gerber et al., 2013; FAO, 2017). Recent studies have revised methane emission estimates from livestock upward by over 10% (Beauchemin et al., 2008; Thornton and Herrero, 2010; Wolf et al., 2017), further emphasizing their critical role in global greenhouse gas budgets (Reisinger and Clark, 2017). Reducing unnecessary greenhouse gas emissions is a global imperative for Earth system management and reducing enteric methane sources is seen as a promising approach to do so (Boadi et al., 2002; DeRamus et al., 2003; Herrero, et al., 2016; Hristov et al., 2013; Johnson and Johnson, 1995; Moss et al., 2000).

Bison in North America are thought to have been responsible for some 2.2 Tg $year^{-1}$ (Kelliher and Clark, 2010; Smith et al., 2016) of the 9-15 Tg $year^{-1}$ of pre-industrial enteric methane emissions (Thompson et al., 1993; Chappellaz et al., 1993; Subak, 1994). Enteric CH_4 emissions from wild ruminants in the United States in the pre-settlement period comprised nearly 90% of current CH_4 emissions from domesticated ruminants assuming an historic bison population size of 50 million

(Hristov, 2012), further demonstrating the importance of bison to methane fluxes in the past. The current and future contribution of non-domesticated ungulates to methane fluxes are uncertain (Crutzen et al., 1985). Previous approaches used inventory approaches or scaling equations that were not derived using methane efflux measurements from bison; the only direct bison methane flux observations that we are aware of measured 30 L per kg dry food intake (17 g methane per kg dry food intake) in one-year-old penned female bison fed alfalfa pellets (Galbraith et al., 1998), more than elk (*Cervus elaphus*) and white-tailed deer (*Odocoileus virginianus*) on a dry matter intake basis and similar to dairy cattle fed high maize silage (Hammond et al., 2016). Cattle methane emissions tend to be greater when fed alfalfa than grass (Chaves et al., 2006) such that existing published values may not represent an accurate estimate of the methane efflux from bison in a natural field setting, which has not been measured to date.

Here, we measure methane flux from a bison herd on winter pasture using the eddy covariance technique (Dengel et al., 2011; Felber et al., 2015; Prajapati and Santos, 2018; Sun et al., 2015). We use flux footprint analyses combined with bison locations determined using automated cameras to estimate methane flux on a per-animal basis and discuss observations in the context of eddy covariance methane flux measurements from other ruminants.

2 Methods

2.1 Study site

The study site is a 5.5-hectare pasture on the Flying D Ranch near Gallatin Gateway, Montana, USA (45.557, −111.229) on a floodplain immediately west of the Gallatin River (Figure 1). Daily high temperatures average 1.6 °C and daily low temperatures average −11.5 °C at Bozeman Yellowstone International Airport (BZN), located 24 km north-northeast of the site, during the November – February measurement period. BZN records an average of 18.2 mm of precipitation per month during November – February, almost entirely as snowfall. A herd of 39 bison entered the pasture on November 17, 2017 and left on February 3, 2018. The mean (standard error) bison weight measured by the landowners on November 16, 2017 before bison entered the pasture was 329 ± 28 kg and the bison varied in age from 0.5 to 7.5 years old (Table S1). Bison consumed a mixture of perennial grasses grown *in situ* that was supplemented by perennial grass hay grown in nearby fields (Table S2) delivered every three days on average (Table S3).

2.2 Instrumentation

A 3 m tower was installed near the center of the study pasture during November 2017 (Figure 1) and surrounded by electric fencing to avoid bison damage. Four game cameras (TimelapseCam, Wingscapes, EBSCO Industries, Inc., Birmingham, AL, USA) were mounted to the tower and pointed in cardinal directions. Two additional game cameras were mounted near the pasture edge facing the tower. Cameras captured images every five minutes and an example of an individual image from the south-facing camera located on the northern edge of the study pasture is shown in Figure 2. Bison locations at the half-

hourly time interval of the eddy covariance measurements were estimated by manually attributing bison locations to squares in a 20 m grid overlaid on the pasture area (Figure 1). The 20 m grid size represents the grid that we felt that we were able to attribute bison locations given features of the field that could be identified by camera. The bison location approach introduces uncertainty, and we test the sensitivity of per-animal methane efflux estimates to bison location estimates as described in the *Spatial Uncertainty* section below.

Incident and outgoing shortwave and longwave radiation and thereby the net radiation were measured using a NR01 net radiometer (Hukseflux, Delft, The Netherlands) mounted 1.5 meters above ground level. A SR50 sonic distance sensor (Campbell Scientific Inc., Logan, UT, USA) was installed at 1.3 m to gauge snow depth, and air temperature and relative humidity were measured at 2.25 meters using a HMP45C probe (Vaisala, Vantaa, Finland). Average 0–30 cm soil moisture and temperature were collected using CS650 probes (Campbell Scientific). Meteorological variables were measured once per minute, and half-hourly averages were stored using a CR3000 datalogger (Campbell Scientific).

Three-dimensional wind velocity was measured using a CSAT-3 sonic anemometer (Campbell Scientific) at 2.0 m above the ground surface. Carbon dioxide mixing ratios were measured at 10 Hz using a LI-7200 closed-path infrared gas analyzer (LI-COR Biosciences, Inc.) with inlet placed at the same height as the center of the sonic anemometer. Methane mixing ratios were measured at 10 Hz using a LI-7700 open-path infrared gas analyzer (LI-COR Biosciences, Inc., Lincoln, NE, USA) with the center of the instrument likewise located at 2.0 m and a 22 cm horizontal offset from the sonic anemometer; open- and closed-path infrared gas analyzers for eddy covariance have similar performance in field settings (Detto et al., 2011; Deventer et al., 2019). We use the atmospheric convention in which flux from biosphere to atmosphere is positive. Measurements were made during winter daytime hours from 0700 to 1700 local time to avoid depleting the battery bank and to ensure sufficient light to estimate bison location using game cameras. Flux measurements began on November 14, 2017 and ended on February 14, 2018.

Bison are dangerous and will charge humans. Their presence complicated data retrieval and game camera upkeep; some high-frequency flux measurements were overwritten and cameras shut down during exceptionally cold periods, resulting in missing measurements. Simultaneous flux and photographic data were obtained for the January 7, 2018 to February 13, 2018 period excluding January 10, 2018 when instruments were obstructed by snowfall. Flux data without accompanying game camera footage were obtained for the periods from November 14 through 29, 2017 and December 31, 2017, through January 6, 2018.

2.3 Flux calculations

Methane and carbon dioxide fluxes were calculated using EddyPro (LI-COR Biosciences, Lincoln, NE, USA). Standard double rotation, block averaging, and covariance maximization with default processing options were applied. Spike removal was performed as described by Vickers and Mahrt (1997) and spikes were defined as more than 3.5 standard deviations from the mean mixing ratio for carbon dioxide and more than 8 standard deviations from the mean mixing ratio for methane given

the expectation of intermittent methane spikes from the bison herd. The default drop-out, absolute limit, and discontinuity tests were applied using the default settings following recommendations by Dumortier et al. (2019), and the Moncrieff et al. (1997) and Moncrieff et al. (2004) low and high-pass filters were applied. The Webb-Pearman-Leuning correction (Webb et al., 1980) was applied to calculate methane efflux using the open-path LI-7700 sensor. Estimates of storage flux in the 2 m airspace below the infrared gas analyzers were assumed to be minor and excluded from the flux calculation. Flux measurements for which the quality control flag was greater than 1 following Mauder and Foken (2004) (see also Foken et al., 2004) were discarded and the net effect of all corrections when bison were present was a methane flux reduction of 14%. Measurements that exceeded an absolute value of 1 μmol m^{-2} s^{-1} for the case of methane flux and 20 μmol m^{-2} s^{-1} for the case of carbon dioxide flux were discarded following an analysis of the probability distribution of observations. We tested the sensitivity of flux measurements to the friction velocity (u^*) to see if measurements made under conditions of insufficient turbulence should be excluded from the analysis despite the daytime-only flux measurement approach.

2.4 Flux footprint modelling

The eddy covariance flux footprint was calculated using the approach of Hsieh et al. (2000) extended to two dimensions following Detto and Katul (2006). Such analytical footprint models have been found to give minimally biased estimates of point-source fluxes in field settings (Dumortier et al., 2019). We performed the footprint analysis on a grid of 1 m pixels and aggregated values to the 20 × 20 m grid to which the bison locations were estimated (Figure 1); Figure 3 demonstrates an example of a flux footprint for a single half-hourly period.

To further characterize the uncertainty in our per-animal methane flux estimates, described next, we also applied the flux footprint parameterization method of Kljun et al. (2015) aggregated to the same 20 × 20 m grid. The Kljun et al. (2015) model performs well in point-source experiments (Heidbach et al., 2017) and is widely used by the flux community.

The momentum roughness height (z_{0m}) is required by both footprint models. Instead of assuming a constant z_{0m} over snow of 0.001 m (Andreas et al., 2004), we followed the approach of Baum et al. (2008) who calculated a unique z_{0m} for each half-hour eddy covariance measurement for a cattle feedlot system by rearranging the wind profile equation:

$$z_{0m} = \frac{z - d}{exp(ku/u_* + \psi_m)} \quad (1)$$

Where z is measurement height, u is wind speed, k is the von Karman constant, and ψ_m is the correction factor for atmospheric stability, here following Brutsaert (1982). The zero-plane displacement (d) for a field with obstacles is calculated following Verhoef et al. (1997):

$$d = z - \frac{z\left(1-\exp\left(-\sqrt{42\alpha}\right)\right)}{\sqrt{42\alpha}}. \quad (2)$$

where a is the frontal area index of the obstacles (Raupach, 1994), here bison:

$$a = \frac{nbh}{s}. \quad (3)$$

The calculation of a uses the number of animals (n = 39), the size of the pasture (S, m^2), and the average breadth (b, m) and height (h, m) of the animals. We used established relationships for beef cattle as a function of weight (ASABE, 2006) given the lack of similar equations for bison. h was adjusted upward by 50% such that the height of adult males better-matched average values of fully-grown bison on the order of 1.8 m. The methane source location was assumed to be near the ground per the typical posture of bison assuming that most methane efflux in ruminants is from eructation.

2.5 Per-bison methane flux estimation

Given that mean methane emissions were not significantly different from zero in the absence of bison – as detailed in *Results* – we assume that observed methane emissions are due to bison in the flux footprint. The relative contribution of bison to each half-hourly eddy covariance measurement was calculated by expanding the approach of Dumortier et al. (2019) (see also Prajapati and Santos (2019)) for multiple point sources. From the definition of the footprint function, the measured density of a scalar X, F_X, for our study area of 8 × 12 grid cells (Figure 1) is:

$$F_X = \sum_{i=1}^{8}\sum_{j=1}^{12} F_{ij}\phi_{ij}\Delta x_{ij}\Delta y_{ij} \tag{4}$$

where ϕ_{ij} is the value of the footprint function in grid cell ij (here per 400 m^2) and x and y are the dimensions of the 20 m grid cells. Dumortier et al. (2019) considered a known point source from a single cell, f_X, such that:

$$f_X = \frac{F_X}{\phi_{ij,source}} \tag{5}$$

where $\phi_{ij,source}$ is the value of the footprint function at the source location. We have n = 39 sources (i.e. bison) that are free to wander to any grid cell ij. We also have no basis for identifying individual bison given the resolution of the cameras, noting that this is possible using higher-resolution cameras (Merkle and Fortin, 2013) or GPS instruments. We also have no basis for determining if the methane sources of individual bison are different using our approach, so we must assume that methane efflux from each bison is equal. Under these assumptions we can write:

$$\langle f_x \rangle = \frac{F_X}{\sum_{i=1}^{8}\sum_{j=1}^{12} n_{ij}\phi_{ij}\Delta x_{ij}\Delta y_{ij}} \tag{6}$$

Where n_{ij} is the number of bison in grid cell ij (i.e. per 400 m^{-2}) and $\langle f_x \rangle$ is the average flux per bison. We only adopt this approach for calculating average methane efflux per bison as measured carbon dioxide fluxes in the absence of bison were greater than zero. Methane efflux values less than −200 μmol bison^{-1} s^{-1} and greater than 300 μmol bison^{-1} s^{-1} were treated as outliers and excluded based on an analysis of the probability distribution of observations.

2.6 Spatial uncertainty

The location of bison in the pasture was approximated visually by identifying the position of bison in relation to static cues in the study area using five-minute photographs. Observations were then aggregated to half-hourly flux measurement

periods. This approach results in spatial uncertainty in bison location, especially due to movements within half-hourly periods and due to the size of the animals themselves with reference to the grid (Figure 1). Both will result in a greater spatial distribution of bison locations than represented in the maps of bison distributions that were created. To arrive at a conservative estimate of uncertainty in per-bison methane flux estimates, we explored the sensitivity of flux estimates to maps of bison location that were more distributed in space. To do so we used two-dimensional Tikhonov Regularization (Tikhonov and Arsenin, 1977), a classic mathematical technique to solve ill-posed problems, here the challenge of estimating the best spatial distribution of bison with intermittent observations.

To briefly describe the motivation for using Tikhonov Regularization for our case, consider the extreme distributions of potential bison locations: all are located in a single grid cell (a Dirac delta function) or all are perfectly aggregated across the field (an uninformed prior). The true distribution likely exists between these cases, especially given intermittent bison movements. The estimates of their location using cameras provides an initial guess of the true location. We assume that the true number of each bison in each pixel is likely to be similar to those measured in adjacent pixels because the bison movements were usually minor and because of the uncertainty that exists when attempting to associate bison to a particular pixel. Two-dimensional Tikhonov Regularization can provide an estimate of the true distribution of elements (here bison) given the constraints that the distribution is bounded and that adjacent pixels are likely similar to a given pixel (Stoy and Quaife, 2015).

We use a form of Tikhonov Regularization to create spatial disaggregation of each bison distribution map (α') following Stoy and Quaife (2015):

$$\alpha' = \alpha(I + \gamma^2 B^T B)^{-1} \frac{\sigma^2}{\psi(\gamma^2)} - \mu_\alpha + \mu_{\alpha'}. \quad (7)$$

Here, α is the measured distribution map with mean μ_α (the number of bison per pixel) and variance σ, I is the identity matrix, B represents the constraint that neighboring elements should be similar by requiring a first difference of zero in the cardinal directions of the map, γ is the Lagrange Multiplier, and $\psi(\gamma^2)$ is a normalization term equal to the variance of $\alpha(I + \gamma^2 B^T B)^{-1}$. Large values γ constrain each pixel to be near the overall mean such that the bison distribution map is smoother across space.

We applied the Tikhonov Regularization approach to each bison distribution map using Lagrange multipliers that ranged from 0.1 to 4 as demonstrated for a single half-hour period in Figure 4; note that the simulation with a Lagrange multiplier of 4 results in a simulation where bison are widely distributed across segments of the field and amounts to a highly conservative estimate of their location. Our results are subject to simultaneous uncertainties in footprint and bison location in addition to the eddy covariance methane flux measurements themselves, which range from 6 – 41% for half-hourly fluxes and 7 – 17% for long-term sums (Deventer et al., 2019). We use 17% as a representative uncertainty of eddy covariance sums as we are primarily concerned with providing a conservative assessment of uncertainty using our approach. We suggest strategies for reducing uncertainty in the *Discussion* section.

3. Results

3.1 Meteorology

Air temperature averaged −2.8 °C and soil temperature averaged −0.3 °C during the measurement period (Figure 5A). Incident shortwave radiation ranged between 100 and 400 W m^{-2} during peak daylight hours (1000-1400 hours local time) across the study period, and clear conditions were common except for four weeks beginning in mid-December (Figure 5B). Snow depth within the tower enclosure increased from 0.15 m to nearly 0.4 m in late 2017 and decreased to 0.1 m beginning in late January 2018 (Figure 5C) noting that snow outside of the electrified tower enclosure was often trampled (see Figure 2). The mean (median) wind direction was 221° (208°) during periods when visible imagery of bison locations was available and eddy covariance measurements passed quality control checks (Figure 6).

3.2 Gas flux

Half-hourly methane fluxes averaged 0.048 ± 0.081 μmol m^{-2} s^{-1} (mean ± standard deviation) and carbon dioxide fluxes averaged 1.6 ± 1.4 μmol m^{-2} s^{-1} when bison were present (Figure 7), noting again that measurements were made only during daytime periods. Methane flux in the absence of bison averaged −0.0009 ± 0.008 μmol m^{-2} s^{-1} and carbon dioxide flux averaged 0.64 ± 1.0 μmol m^{-2} s^{-1}, significantly lower than when bison were present ($P < 0.001$ for both CH_4 and CO_2). CO_2 flux was significantly related to methane flux and explained 52% of its variance when bison were present but only 7% when they were absent (Figure 8). CO_2 flux was significantly and positively related to air and soil temperature across the entire measurement record ($P < 0.001$ in both cases), but methane flux was not. There were no significant temporal patterns of methane flux during the daytime periods investigated here, and neither incident nor net radiation were related to methane fluxes. When bison were present, methane flux was not significantly different at the $P < 0.05$ significance level during days when feed was delivered (0.051 ± 0.083 μmol m^{-2} s^{-1}) and days when it was not (0.035 ± 0.10 μmol m^{-2} s^{-1}) ($P = 0.075$).

Methane flux was significantly and positively related to friction velocity in the absence of bison at u^* values greater than 0.2 m s^{-1} ($P = 0.003$) but not positively related to u^* values less than 0.2 m s^{-1}, indicating that flux measurements were unrelated to friction velocity values commonly associated with insufficient turbulence (Figure 9A). Carbon dioxide flux was not related to u^* in the absence of bison (Figure 9B) but negative values were observed at u^* values greater than 0.45 m s^{-1}. Given these observations, we did not apply a u^* filter to our eddy covariance measurements, which were made only during daytime periods. We discuss potential reasons for the observed increase in methane flux and negative CO_2 flux with high values of u^* in the *Discussion* section.

3.3 Bison location and methane efflux

Timelapse camera footage yielded usable imagery for 444 half-hourly periods of which 245 half-hourly periods had available eddy covariance observations and of which 177 had eddy covariance measurements that passed quality control criteria. Bison tended to aggregate in an area on the west side of the pasture near the location where supplemental hay was

often provided (Figure 10A). They intermittently visited the area north of the tower in mornings and afternoons and intermittently made sporadic mass movements to the southernmost edge of the field near its gate during midday periods (Figure 10B-D).

Bison were located within the 90% flux footprint 40% of the time (Figure 11). There was an average of eight (seven bison within the 90% flux footprint of the Hiseh et al. (2000) (Kljun et al. (2015)) models whichh increased to both footprint models which increased to 21 (20), respectively, when excluding observations with no bison (Figure 11). Per-bison methane emission estimates when using the Hsieh et al. (2000) footprint model had a mean (± standard error) of 55 ± 0.96 μmol bison^{-1} s^{-1} and a median of 29 μmol bison^{-1} s^{-1} as a result of the positively skewed measurement distribution (Figure 12A). These estimates are 11% lower than per-bison methane emission estimates from the Kljun et al. (2015) footprint model, which returned a mean (± standard error) of 62 ± 0.91 μmol bison^{-1} s^{-1}, which demonstrates that per-animal flux estimates are sensitive to flux footprint methodology. Per-animal flux estimates are also sensitive to the estimates of their location within the field; mean methane flux estimates ranged from 43 – 58 μmol bison^{-1} s^{-1} when applying the Hsieh et al. (2000) model and 50 – 75 μmol bison^{-1} s^{-1} when applying the Kljun et al. (2015) model after spatial smoothing using Tikhonov Regularization. These estimates are up to 22% different than the mean methane flux estimates that were generated by taking the maps at face value. If we adopt 22% as a conservative uncertainty estimate due to spatial uncertainty and 17% as a conservative uncertainty estimate of long-term methane flux sums (Deventer et al., 2019) for a combined uncertainty of 28%, we arrive at a daily per-bison methane flux estimate of 76 ± 21 g CH_4 bison^{-1} day^{-1} when using the Hsieh et al. (2000) footprint model and 86 ± 24 g CH_4 bison^{-1} day^{-1} when using the Kljun et al. (2015) footprint model.

4 Discussion

The eddy covariance flux footprint analysis coupled to bison location estimates from automated camera images resulted in a mean (median) methane flux of 55 (29) μmol bison^{-1} s^{-1} when applying the Hsieh et al. (2000) footprint model and 62 (43) μmol bison^{-1} s^{-1} when applying the Kljun et al. (2015) footprint model. Measurements were made during daytime periods in winter and are sensitive to estimates of bison location (Figure 12). If we naively assume that methane flux from bison varies negligibly across the full diurnal and seasonal range, a notion that needs to be substantiated, our measurements with conservative uncertainty estimates correspond to 26 ± 8 (31 ± 9) kilograms of methane per bison per year when applying the Hsieh et al. (2000) (Kljun et al. (2015)) model, noting that methane emissions from cattle have been observed to be on the order of 10-17% higher in summer than winter (Todd et al., 2014; Prajapati and Santos, 2018; Prajapati and Santos, 2019) but lower in evenings if animals eat less during these times (Gao et al., 2011). The mean weight of the study bison herd was 329 kg, similar to the 300 kg buffalo that is assumed to emit 55 kg year^{-1} in the 2006 IPCC report (IPCC 2006) noting that dairying buffalo cows are estimated to have higher methane emissions than other buffalo (Cóndor et al. 2008). The study herd here comprised numerous pregnant females (Table S1) that have higher metabolic requirements. Previous estimates of methane emissions from range cattle are on the order of 60 kg per year per animal (Hogan, 1993), about twice as large as the mean per-bison methane flux calculated here. Values were instead similar to the lower range measurements from young

heifers feeding on ryegrass of 88 g CH_4 $animal^{-1}$ day^{-1} (Hammond et al., 2016) and wintertime measurements of beef cattle in a feedlot on the order of 75 g CH_4 $animal^{-1}$ day^{-1} (Prajapati and Santos, 2019). In other words, while there is no evidence from our measurements that bison have more or less methane efflux than typical values reported for cattle, it is critical to make full year-round methane flux measurements with uncertainty to understand the seasonal course of bison methane efflux to establish defensible annual sums.

Below, we discuss potential reasons for the relatively low bison methane emissions observed here as well as a strategy for reducing uncertainty in eddy covariance measurements of methane efflux from grazing non-domesticated ruminants.

4.1 Bison methane and carbon dioxide efflux in response to environmental variables

Methane flux was not related to air or soil temperature but was related to u^* – especially at relatively high values of u^* – in the absence of bison (Figure 9). These observations are consistent with a potential pressure pumping mechanism for trace gases through snow at higher wind speeds (Bowling and Massman, 2011) although it is unclear why this relationship exists for methane flux and not carbon dioxide flux as is frequently found in snow-covered conditions (Rains et al., 2016). Carbon dioxide flux at high values of u^* was negative indicating net CO_2 uptake by the biosphere, which is unlikely in our study site during winter, suggesting that values with excessively high u^* may need to be filtered, but with only five observations of CO_2 flux less than zero it is unclear how to apply such a filter in our case.

Insufficient evidence exists in our data record to attribute observed methane efflux to the onset of freezing conditions in soil (Mastepanov et al., 2008). We note that extensive snow trampling (e.g., Figure 2) likely resulted in a situation where snow depth (Figure 5C) and its insulating effect on soil temperature (Figure 5A) varied across the field and therefore differed from snow and soil measurements taken within the instrumentation enclosure. Regardless, mean methane flux when bison were absent, -0.0009 μmol m^{-2} s^{-1}, was nearly two orders of magnitude less than the mean methane flux when bison were present, 0.041 μmol m^{-2} s^{-1}. Whereas we cannot exclude – and in fact expect – positive and negative background methane fluxes from non-bison sources in a grassland in winter in the vicinity of a riparian area (Figure 1, Merbold et al., 2013; McLain and Martens, 2006; Mosier et al., 1991), these appear to be minor compared to the CH_4 flux attributable to bison (Figures 7 and 8). Bison are associated with a distinct methane flux signature as shown by the immediate decline of methane fluxes following their removal from the study pasture (Figure 7) and strong relationship with carbon dioxide flux (Figure 8) given the common source of respiration and most enteric methane losses from the mouths of ungulates. Methane flux was related to carbon dioxide flux when bison were present or absent (Figure 8), suggesting both soil and ruminant sources (and in the case of methane sinks) of both gases (Baldocchi et al., 2012; Motte et al., 2019).

It is important to note that potential methane fluxes from bison manure may have been dampened by freezing conditions but are an important methane source during warmer conditions in ruminant grazing systems (Dengel et al., 2011). Manure is thought to contribute a nontrivial portion (10-14 Tg CH_4 yr^{-1}) of total global ruminant methane efflux (77 Tg CH_4 yr^{-1}, Johnson and Ward 1996; Moss et al., 2000) noting that some farm-scales studies arrive at lower percentages (Taylor et al.,

2017). Though we did not observe higher methane efflux early in the study period when soil temperature was above freezing nor temperature sensitivity of methane efflux in the presence or absence of bison, it is important to note that field-scale methane efflux may be diminished by the thermal environment of manure in our measurements such that methane efflux is lower than would be expected during warmer seasons.

4.2 Bison spatial distribution and movement

Ruminant behavior is critical to track to estimate field-scale efflux (de la Motte et al., 2019). The spatial distribution of bison in the study pasture varied from morning to midday and afternoon (Figure 10). It is difficult to infer from the available data whether the study bison are more active during morning and evening hours in the pasture environment like cattle (Gregorini 2012). Supplemental hay was made available to the bison approximately 50 meters west of the tower and increases in the frequency of bison appearance there are likely associated with the animals' preferred feeding times after dawn and before dusk, but observed methane flux did not vary as a function of time of day (e.g. Dengel et al. 2011) and was not significantly different during days when hay was provided and when it was not, noting that the animals were free to also graze on vegetation within the pasture. Regardless, ruminant methane flux measurements are simpler to make when animals congregate (Coates et al., 2017; Tallec et al., 2012) as was often observed here (e.g. Figures 2, 10 & 11). Aggregation behavior in our study bison herd was often upwind of the eddy covariance tower (Figures 6 & 10) and resulted in more overlap between flux footprint and bison location than would have occurred if bison locations were randomly distributed throughout the study area, emphasizing the importance of tower placement in eddy covariance studies of grazing systems.

Spatial uncertainties in bison location interact with uncertainties in flux footprint modelling for methane source attribution (Figure 12). Footprint models of the type used here have been found to accurately estimate point sources of trace gas flux (Heidbach et al., 2017; Dumortier et al., 2019), but it is important to note that footprint modelling techniques play a large role in the spatial attribution of observed fluxes of ruminant trace gas flux (Felber et al., 2015). Prajapati and Santos (2018), for instance, found that an analytical model (Kormann and Meixner 2001) predicted flux footprint areas five to six times larger than did an approximation of a Lagrangian dispersion model (Kljun et al., 2002), such that footprint model uncertainty is a major source of uncertainty for measuring methane flux from multiple point sources as we also found here.

4.3 Future directions for greenhouse gas accounting in ruminant grazing systems

Methane efflux cannot be completely removed from ruminant grazing systems; some 4.6 – 6.2% of gross energy intake is lost as methane in cattle, sheep and goats worldwide (Johnson and Ward 1996) with cattle often falling on the higher end of the observed range (Lassey et al., 1997). But there are other aspects of bison ecology that merit consideration when designing greenhouse gas-cognizant grazing systems. For example, cattle tend to graze close to water more frequently than bison do (Allred et al., 2011) with unclear consequences for riparian vegetation, water quality, and potential methane efflux

from cattle wallows. Cattle also tend to graze for longer periods than bison (Plumb and Dodd, 1993) and it is unclear if there is an associated consequence for methane efflux. Future work should consider the large inter-animal variability in methane efflux (Lassey et al., 1997), possibly using advanced techniques for identifying individual animals through photographs (Merkle and Fortin, 2013) or tracking devices (Felber et al., 2015). Animal age and size are also important factors in ruminant methane efflux (Jiao et al., 2014) and individual tracking may improve our estimates of this variability in a field setting.

Adding seasonal foraging behavior, estimating emissions from individual animals, and addressing seasonal and inter-annual variability and trends in forage nutrition are likely to further improve prediction of methane emissions from grazing systems (Moraes et al., 2013). Advanced eddy covariance algorithms for are also likely to improve flux estimates on short time scales noting that non-stationary bursts have not been found to create systematic bias in methane budgets measured over longer time periods using eddy covariance (Göckede et al., 2019). Of these, advanced footprint attribution techniques like Environmental Response Functions designed to create improved maps of surface-atmosphere fluxes (Metzger et al., 2013; Xu et al., 2017) may be uniquely applicable to the challenging case presented by grazing systems with mobile point sources and intermittent biogeochemical hotspots created by animal waste. Going forward, increases in atmospheric carbon dioxide concentrations are likely to decrease forage quality (Jégo et al., 2013), resulting in higher leaf carbon to nitrogen ratios and which is expected to increase ruminant methane emissions (Lee et al., 2017), all else being equal. Understanding greenhouse gas fluxes from ruminants is therefore likely to be even more important in the future. An ongoing interest in bison reintroduction and ungulate ecology coupled with established micrometeorological measurement techniques will help us understand the present and future role that bison and alternative grazing systems play in the Earth system.

Supplemental Information

The land managers provided information that describes bison age, sex, weight, and pregnancy status (Table S1) and the composition (Table S2) and the delivery schedule (Table S3) of hay.

Acknowledgements

PCS acknowledges support from the U.S. National Science Foundation awards DEB-1552976 and OIA-1632810, the USDA National Institute of Food and Agriculture Hatch project 228396, the Multi-State project W3188, the Graduate School at Montana State University, and the University of Wisconsin – Madison. Funding for the LI-7700 methane analyzer used in this work was provided to JED by NSF-EPSCoR award EPS-1101342 and Montana State University. Daniel Salinas, Gabriel Bromley, Zheng Fu, and James Irvine provided technical assistance. This work could not have been completed without permission of Turner Enterprises, Inc. and the assistance of Carter Kruse and Danny Johnson.

Code/Data availability

Eddy covariance and micrometeorological data have been submitted to Ameriflux for publication at https://ameriflux.lbl.gov/sites/siteinfo/US-Tur.

Author contributions

PCS designed the study with AC, JD, and WK and wrote the manuscript with all coauthors. AC collected data and analyzed it with PCS and TG. NK assisted with the footprint analysis.

Competing interests

The authors declare no competing interests.

References

Allred, B. W., Fuhlendorf, S. D. and Hamilton, R. G.: The role of herbivores in Great Plains conservation: comparative ecology of bison and cattle. Ecosphere 2(3), 26, 2011.

Andreas, E. L., Jordan, R. E., Guest, P. S., Persson, O. G., Grachev, A. A., and Fairall, C. W.: Roughness lengths over snow. In 18th Conference on Hydrology of the American Meteorological Society, Seattle, WA, 11–15 January, 2004.

Baldocchi, D. D., Detto, M., Sonnentag, O., Verfaillie, J., Teh, Y. A., Silver, W. and Kelley, N. M.: The challenges of measuring methane fluxes and concentrations over a peatland pasture. Agric. For. Met. 153, 177-187, 2012.

Baum, K. A., Ham, J. M., Brunsell, N. A. and Coyne, P. I.: Surface boundary layer of cattle feedlots: Implications for air emissions measurement. Ag. Forest. Met. 148, 1882-1893, 2008.

Beauchemin, K. A., Kreuzer, M., O'Mara, F. and McAllister, T. A.: Nutritional management for enteric methane abatement: a review, Aust. J. Exp. Agric., 48(2), 21–27, 2008.

Boadi, D. A. and Wittenberg, K. M.: Methane production from dairy and beef heifers fed forages differing in nutrient density using the sulphur hexafluoride (SF_6) tracer gas technique. Can. J. Anim. Sci., 82, 201-206, 2002.

Bowling, D. R. and Massman, W. J.: Persistent wind-induced enhancement of diffusive CO_2 transport in a mountain forest snowpack. J. Geophys. Res. 116, 1–15, 2011.

Brutsaert, W.: Evaporation into the Atmosphere: Theory, History, and Applications. Dordrecht: Kluwer, 1982.

Chappellaz, J. A., Fung, I. Y. and Thompson A. M.: The atmospheric CH_4 increase since the Last Glacial Maximum. Tellus B, 45(3), 228-241, 1993.

Chaves, A. V., Thompson, L., C., Iwaasa, A., D., Scott, S., L., Olson, M. E., Benchaar, C., Veira, D., M. and McAllister, T., A.: Effect of pasture type (alfalfa vs. grass) on methane and carbon dioxide production by yearling beef heifers. Can. J. Anim. Sci., 86, 409-418, 2006.

Coates, T., W., Benvenutti, M. A., Flisch, T. K., Charmley, E., McGinn, S. M. and Chen D.: Applicability of eddy covariance to estimate methane emissions from grazing cattle. J. Environ. Qual. 47(1), 54-61, 2017.

Collins, S.L. and Steinauer, E.M.: Disturbance, diversity and species interactions in tallgrass prairie. In: Knapp AK, Briggs JM, Hartnett DC, Collins SC (ed) Grassland Dynamics: Long-Term Ecological Research in Tallgrass Prairie. Oxford University Press, pp 140–156, 1998.

Cóndor, R. D., Valli, L., De Rosa, G., Di Francia, A. and De Lauretis, R: Estimation of the methane emission factor for the Italian Mediterranean buffalo. Animal 2:8, 1247–1253, 2008.

Coppedge, B. R. and Shaw, J. H.: Bison grazing patterns on seasonally burned tallgrass prairie. J. Range Manage. 51, 258-264, 1998.

Crutzen, P. J., Aselmann, I. and Seiler, W.: Methane production by domestic animals, wild ruminants, other herbivorous fauna, and humans. Tellus B 38, 271-284, 1985.

de la Motte, L. G., Dumortier, P., Beckers, Y., Bodson, B., Heinesch, B. and Aubinet, M.: Herd position habits can bias net CO_2 ecosystem exchange estimates in free range grazed pastures, Agric. For. Met. 268, 156–168, 2019.

Dengel, S., Levy, P. E., Grace, J., Jones, S. K. and Skiba, U. M.: Methane emissions from sheep pasture, measured with an open-path eddy covariance system, Glob. Chang. Biol. 17(12), 3524–3533, 2011.

DeRamus, H.A., Clement, T.C., Giampola, D.D. and Dickison, P.C.: Methane emissions of beef cattle on forages. J. Environ. Qual.: 32(1), 269-277, 2003.

Detto, M. and Katul, G. G.: Simplified expressions for adjusting higher-order turbulent statistics obtained from open path gas analyzers, Bound.-Layer Meteorol., 122(1), 205–216, 2006.

Detto, M., Verfaillie, J., Anderson, F., Xu, L. and Baldocchi, D.: Comparing laser-based open- and closed-path gas analyzers to measure methane fluxes using the eddy covariance method, Agric. For. Meteorol., 151(10), 1312–1324, 2011.

FAO: Global Livestock Environmental Assessment Model (GLEAM). Rome, 2017.

Deventer, M. J., Deventer, M., Griffis, T. J., Roman, D., Kolka, R. K., Wood, J. D., Erickson, M., Baker, J. M. and Millet, D. B.: Error characterization of methane fluxes and budgets derived from a long-term comparison of open- and closed-path eddy covariance systems, Agricultural and Forest Meteorology, 278, 107638, 2019.

Dumortier, P., Aubinet, M., Lebeau, F., Naiken, A. and Heinesch, B.: Point source emission estimation using eddy covariance: Validation using an artificial source experiment. Agric. For. Meteorol., 266-267, 148-156, 2019.

Felber, R., Münger, A., Neftel, A. and Ammann, C.: Eddy covariance methane flux measurements over a grazed pasture: effect of cows as moving point sources, Biogeosciences, 12(12), 3925–3940, 2015.

Flores D: Bison ecology and bison diplomacy: The southern plains from 1800 to 1850. J Am Hist 78:465–485, 1991.

Fortin, D., Fryxell, J. M., O'Brodovich, L. and Frandsen, D.: Foraging ecology of bison at the landscape and plant community levels: the applicability of energy maximization principles, Oecologia, 134(2), 219–227, 2003.

Freese, C. H., Aune, K. E., Boyd, D. P., Derr, J. N., Forrest, S. C., Gates, C. C., Gogan, P. J. P., Grassel, S. M., Halbert, N., D., Kunkel, K. and Redford, K., H.: Second chance for the plains bison. Biological Conservation, 136(2), 175-184, 2007.

Galbraith, J. K., Mathison, G. W., Hudson, R. J., McAllister, T. A. and Cheng, K.-J.: Intake, digestibility, methane and heat production in bison, wapiti and white-tailed deer, Can. J. Anim. Sci., 78(4), 681–691, 1998.

Foken T., Göckede, M., Mauder, M., Mahrt, L., Amiro, B. and Munger W.: Post-field data quality control. In Lee, X., Massman, W.J. and Law, B. (eds) Handbook of micrometeorology: A guide for surface flux measurement and analysis. Kluwer, Dordrecht, The Netherlands, 2004.

Gates, C. C., Freese, C. H., Gogan, P. J. and Kotzman M (eds): American bison: status survey and conservation guidelies 2010. IUCN, 2010.

Gerber, P.J., Steinfeld, H., Henderson, B., Mottet, A., Opio, C., Dijkman, J., Falcucci, A. and Tempio, G.: Tackling climate change through livestock - A global assessment of emissions and mitigation opportunities. Food and Agriculture Organization of the United Nations (FAO), Rome, 2013.

Geremia, C, Merkle, J.A., Eaker, D.R., Wallen, R.L., White, P.J., Hebblewhite, M. and Kaufman, M.J.: Migrating bison engineer the green wave. Proc. Nat. Acad. Sci.: 116(51), 25707-25713, 2019.

Gregorini, P. Diurnal grazing pattern: its physiological basis and strategic management. Animal Production Science 52.7: 416-430, 2012.

Göckede, M., Kittler, F. and Schaller, C.: Quantifying the impact of emission outbursts and non-stationary flow on eddy-covariance CH_4 flux measurements using wavelet techniques, Biogeosciences, 16, 3113–3131, 2019.

Hammond, K.J., Jones, A.K., Humphries, D.J., Crompton, L.A. and Reynolds, C.K.: Effects of diet forage source and neutral detergent fiber content on milk production of dairy cattle and methane emissions determined using GreenFeed and respiration chamber techniques. J. Dairy Sci. 99: 7904-7917, 2016.

Hanson, J.R.: Bison ecology in the Northern Plains and a reconstruction of bison patterns for the North Dakota region. Plains Anthropol., 93–113, 1984.

Hartnett, D.C., Hickman, K.R. and Fischer, W.L.E.: Effects of bison grazing, fire, and topography on floristic diversity in tallgrass prairie. J. Range. Manage., 49, 413-420, 1996.

Hedrick, P. W.: Conservation genetics and North American bison (*Bison bison*), J. Hered., 100(4), 411–420, 2009.

Hogan, K. B.: Anthropogenic methane emissions in the United States: Estimates for 1990. National Service Center for Environmental Publications, 1993.

Herrero, M., Henderson, B., Havlík, P., Thornton, P. K., Conant, R. T., Smith, P., Wirsenius, S., Hristov, A. N., Gerber, P., Gill, M., Butterbach-Bahl, K., Valin, H., Garnett, T. and Stehfest, E.: Greenhouse gas mitigation potentials in the livestock sector, Nature Climate Change, 6(5), 452–461, doi:10.1038/nclimate2925, 2016.

Heidbach, K., Schmid, H.-P., and Mauder, M.: Experimental evaluation of flux footprint models. Agric. For. Meteorol. 246: 142-153.

Hristov, A.N.: Historic, pre-European settlement, and present-day contribution of wild ruminants to enteric methane emissions in the United States. J. Animal Sci.: 90(4), 1371-1375, 2012.

Hristov, A. N., Oh, J., Firkins, J. L., Dijkstra, J., Kebreab, E., Waghorn, G., Makkar, H. P. S., Adesogan, A. T., Yang, W., Lee, C., Gerber, P. J., Henderson, B. and Tricarico, J. M.: Special topics — Mitigation of methane and nitrous oxide

emissions from animal operations: I. A review of enteric methane mitigation options, Journal of Animal Science, 91(11), 5045–5069, doi:10.2527/jas.2013-6583, 2013.

Hsieh, C.-I., Katul, G. and Chi, T.-W.: An approximate analytical model for footprint estimation of scalar fluxes in thermally stratified atmospheric flows, Adv. Water Resour., 23(7), 765–772, 2000.

Intergovernmental Panel on Climate Change: Emissions from livestock and manure management. *2006 IPCC guidelines for national greenhouse gas inventories*, 2006.

Isenberg, A.C. The Destruction of the Bison: An Environmental History, 1750–1920. Cambridge Univ Press, Cambridge, UK, 2000.

Jégo, G., Bélanger, G., Tremblay, G. F., Jing, Q. and Baron, V. S.: Calibration and performance evaluation of the STICS crop model for simulating timothy growth and nutritive value, Field Crops Res., 151, 65–77, 2013.

Jiao, H., Yan, T., Wills, D. A., Carson, A. F. and McDowell, D. A.: Development of prediction models for quantification of total methane emission from enteric fermentation of young Holstein cattle at various ages. *Agriculture, Ecosystems & Environment*, *183*, 160-166, 2014.

Johnson, K. A. and Johnson, D. E.: Methane emissions from cattle. J. Anim. Sci., 73, 2483-2491, 1995.

Johnson, D. E. and Ward, G. M.: Estimates of animal methane emissions. Environ. Monit. Assess., 42, 133-141, 1996.

Kelliher, F. M. and Clark, H.: Methane emissions from bison—An historic herd estimate for the North American Great Plains, Agric. For. Meteorol., 150(3), 473–477, 2010.

Kirschke, S., Bousquet, P., Ciais, P., Saunois, M., Canadell, J. G., Dlugokencky, E. J., Bergamaschi, P., Bergmann, D., Blake, D. R., Bruhwiler, L., Cameron-Smith, P., Castaldi, S., Chevallier, F., Feng, L., Fraser, A., Heimann, M., Hodson, E. L., Houweling, S., Josse, B., Fraser, P. J., Krummel, P. B., Lamarque, J.-F., Langenfelds, R. L., Le Quéré, C., Naik, V., O'Doherty, S., Palmer, P. I., Pison, I., Plummer, D., Poulter, B., Prinn, R. G., Rigby, M., Ringeval, B., Santini, M., Schmidt, M., Shindell, D. T., Simpson, I. J., Spahni, R., Steele, L. P., Strode, S. A., Sudo, K., Szopa, S., van der Werf, G. R., Voulgarakis, A., van Weele, M., Weiss, R. F., Williams, J. E. and Zeng, G.: Three decades of global methane sources and sinks, Nat. Geosci., 6(10), 813–823, 2013.

Kljun, N., Rotach, M.W., Schmid, H.P.: A 3D Backward Lagrangian Footprint Model for a Wide Range of Boundary Layer Stratifications. Boundary-Layer Meteorology 103, 205-226, 2002.

Kljun, N., Calanca, P., Rotach, M.W., Schmid, H.P.: A simple two-dimensional parameterisation for Flux Footprint Prediction (FFP), Geoscientific Model Development, 8, 3695-3713, 2015.

Knapp, A. K., Blair, J. M., Briggs, J. M., Collins, S. L., Hartnett, D. C., Johnson, L. C. and Towne, G. E.: The keystone role of bison in North American tallgrass prairie, Bioscience, 49(1), 39, 1999.

Kormann, R. and Meixner F. X.. An analytical footprint model for non-neutral stratification. Bound.-Layer Meteorol., 99(2), 207-224, 2001.

Lassey, K. R., Ulyatt, M. J., Martin, R. J., Walker, C. F. and Shelton, I., D.: Methane emissions measured directly from grazing livestock in New Zealand. Atmos. Environ. 31, 2905-2914, 1997.

Lee, M. A., Davis, A. P., Chagunda, M. G. G. and Manning, P.: Forage quality declines with rising temperatures, with implications for livestock production and methane emissions, Biogeosciences, 14, 1403-1417, 2017.

Mastepanov, M., Sigsgaard, C., Dlugokencky, E. J., Houweling, S., Ström, L., Tamstorf, M. P. and Christensen, T. R.: Large tundra methane burst during onset of freezing. Nature, 456, 628–631, 2008.

Mauder, M., and Foken, T.: Documentation and instruction manual of the eddy-covariance software package TK3, 2011.

McLain, J.E. and Martens, D.A.: Moisture controls on trace gas fluxes in semiarid riparian soils. Soil Sci. Soc. Am. J. 70(2), 367-77, 2006.

Merbold, L., Steinlin, C. and Hagedorn, F.: Winter greenhouse gas fluxes (CO_2, CH_4 and N_2O) from a subalpine grassland. Biogeosciences. 10(5), 3185-3203, 2013.

Metzger, S., Junkermann, W., Mauder, M., Butterbach-Bahl, K., Trancón y Widemann, B., Neidl, F., Schäfer, K., Wieneke, S., Zheng, X.H., Schmid, H.P. and Foken, T.: Spatially explicit regionalization of airborne flux measurements using environmental response functions. Biogeosciences, 10(4), 2193-2217, 2013.

Merkle, J. A. and Fortin D.: Likelihood-based photograph identification: Application with photographs of free-ranging bison. Wild. Soc. Bull., 38, 196-204, 2014.

Moncrieff, J., Clement, R., Finnigan, J., and Meyers, T.: Averaging, detrending, and filtering of eddy covariance time series. In Lee, X., Massman, W.J. and Law, B. (eds) Handbook of Micrometeorology. Springer, Dordrecht, 7-31, 2004.

Moncrieff, J.B., Massheder, J.M., De Bruin, H., Elbers, J., Friborg, T., Heusinkveld, B., Kabat, P., Scott, S., Søgaard, H., and Verhoef, A.: A system to measure surface fluxes of momentum, sensible heat, water vapour and carbon dioxide. J. Hydrology, 188, 589-611, 1997.

Moraes, L. E., Strathe, A. B., Fadel, J. G., Casper, D. P. and Kebreab, E.: Prediction of enteric methane emissions from cattle. Glob. Change Biol., 20, 2140-2148, 2014.

Moe, P. W. and Tyrrell, H. F.: Methane production in dairy cows, J. Dairy Sci., 62(10), 1583–1586, 1979.

Mosier, A., Schimel, D., Valentine, D., Bronson, K. and Parton, W. Methane and nitrous oxide fluxes in native, fertilized and cultivated grasslands. Nature, 350(6316), 330-332, 1991.

Moss, A.R., Jouany, J.-P., and Newbold, J.: Methane production by ruminants: its contribution to global warming. Ann. Zootech., 49, 231-253, 2000.

Nisbet, E. G., Manning, M. R., Dlugokencky, E. J., Fisher, R. E., Lowry, D., Michel, S. E., Lund Myhre, C., Platt, S. M., Allen, G., Bousquet, P., Brownlow, R., Cain, M., France, J. L., Hermansen, O., Hossaini, R., Jones, A. E., Levin, I., Manning, A. C., Myhre, G., Pyle, J. A., Vaughn, B. H., Warwick, N. J. and White, J. W. C.: Very strong atmospheric methane growth in the 4 Years 2014–2017: Implications for the Paris Agreement, Glob. Biogeochem. Cycles, 33(3), 318–342, 2019.

Pereira D.: Wind Rose (https://www.mathworks.com/matlabcentral/fileexchange/47248-wind-rose), MATLAB Central File Exchange. Retrieved May 27, 2020.

Plumb, G. E. and Dodd J. L.: Foraging ecology of bison and cattle on a mixed prairie: implications for natural area management. Ecol. App. 3, 631– 643, 1993.

Prajapati, P. and Santos, E. A.: Estimating methane emissions from beef cattle in a feedlot using the eddy covariance technique and footprint analysis, Agric. For. Meteorol., 258, 18–28, 2018.

Rains, F. A., Stoy, P. C., Welch, C. M., Montagne, C. & McGlynn, B. L.: A comparison of methods reveals that enhanced diffusion helps explain cold-season soil CO_2 efflux in a lodgepole pine ecosystem. Cold Regions Science and Technology, 121, 16-24, 2016.

Reisinger, A. and Clark, H.: How much do direct livestock emissions actually contribute to global warming? Glob. Chang Biol. 24(4), 1749-1761, 2018.

Sanderson, E.W., Redford, K.H., Weber, B., Aune, K., Baldes, D., Berger, J., Carter, D., Curtin, C., Derr, J., Bodrott, S., Fearn, E., Fleener, C., Forrest, S., Gerlach, C., Gates, C. C. Gross, J. E., Gogan, P., Grassel, S., Hilty, J.A., Jensen, M., Kunkel, K., Lammers, D., List, R., Minowski, K., Olson, T., Pague, C., Robertson, P. and Stephenson, B.: The ecological future of the North American Bison: Conceiving long-term, large-scale conservation of wildlife, Conservation Biology 22(2), 252-266, 2008.

Smith, F. A., Hammond, J. I., Balk, M. A., Elliott, S., M., Lyons, S., K., Pardi, M., I., Tomé, C. P., Wagner, P., J. and Westover, M., L.: Exploring the influence of ancient and historic megaherbivore extirpations on the global methane budget. Proc. Natl. Acad. Sci. U. S. A., 113 (4), 874-879, 2016.

Smits, D. D.: The frontier army and the destruction of the buffalo: 1865-1883. West. Hist. Q., 25, 313–338, 1994.

Steuter, A. A. and Hidinger, L.: Comparative ecology of bison and cattle on mixed-grass prairie. Great Plains Research 9:329–342, 1999.

Stoy, P. C. and Quaife T.: Probabilistic downscaling of remote sensing data with applications for multi-scale biogeochemical flux modeling. PLoS One, 10(6): e0128935, 2005.

Subak, S.: Methane from the House of Tudor and the Ming Dynasty: Anthropogenic emissions in the sixteenth century. Chemosphere, 29(5), 843-854, 1994.

Sun, K., Tao, L., Miller, D. J., Zondlo, M. A., Shonkwiler, K. B., Nash, C. and Ham, J. M.: Open-path eddy covariance measurements of ammonia fluxes from a beef cattle feedlot, Agric. For. Meteorol., 213, 193–202, 2015.

Tallec, T., Klumpp, K., Hensen, A., Rochette, Y. and Soussana, J.-F.: Methane emission measurements in a cattle grazed pasture: a comparison of four methods. Biogeosciences Discussions, doi.org/10.5194/bgd-9-14407-2012, 2012.

Taylor, A. M., Amiro, B. D., Tenuta, M. and Gervais, M.: Direct whole-farm greenhouse gas flux measurements from a beef cattle operation. Agr. Ecosyst. Environ., 239, 65-79, 2017.

Thompson, A. M., Chappellaz, J. A., Fung, I. Y. and Kucsera, T. L.: The atmospheric CH_4 increase since the Last Glacial Maximum, Tellus B Chem. Phys. Meteorol., 45(3), 242–257, 1993.

Tikhonov, A.N. and Arsenin, V.Y.: Solutions of ill-posed problems. Washington, D.C.: Winston, 1977.

Thornton, P. K. and Herrero, M.: Potential for reduced methane and carbon dioxide emissions from livestock and pasture management in the tropics, Proc. Natl. Acad. Sci. U. S. A., 107(46), 19667–19672, 2010.

Todd, R. W., Altman, M. B., Cole, N. A. and Waldrip, H. M.: Methane emissions from a beef cattle feedyard during winter and summer on the Southern High Plains of Texas, J. Environ. Qual., 43, 1125-1130, 2014.

Towne, E.G., Hartnett, D.C., Cochran, R.C.: Vegetation trends in tallgrass prairie from bison and cattle grazing, Ecol. Appl., 15, 1550–1559, 2005.

Vickers, D. and Mahrt, L.: Quality control and flux sampling problems for tower and aircraft data, J. Atmos. Ocean. Technol., 14(3), 512–526, 1997.

Vinton, M. A., Hartnett, D. C., Finck, E. J. and Briggs, J. M.: Interactive effects of fire, bison (*Bison bison*) grazing and plant community composition in tallgrass prairie, Am. Midl. Nat., 129(1), 10, 1993.

Webb, E. K., Pearman, G. I. and Leuning, R.: Correction of flux measurements for density effects due to heat and water vapour transfer, Quarterly Journal of the Royal Meteorological Society, 106(447), 85–100, 1980.

Wolf, J., Asrar, G. R. and West, T. O.: Revised methane emissions factors and spatially distributed annual carbon fluxes for global livestock, Carbon Balance Manag., 12(1), 16, 2017.

Xu, K., Metzger, S. and Desai, A.R.: Upscaling tower-observed turbulent exchange at fine spatio-temporal resolution using environmental response functions. Agric. For. Meteorol., 232, 10-22, 2017.

Zontek, K.: Buffalo Nation: American Indian Efforts to Restore the Bison, Bison Books., 2007.

Tables

Table S1: The sex, age, and pregnancy status of the study bison with weight measured on November 16, 2017 shortly before they entered the pasture on November 17, 2017. Bison were assumed to be born on June 1 of the birth year by the landowners such that animals born in 2017 were nearly 6 months old when measurements began.

Sex	Age	Weight (kg)	Pregnant
F	7.5	467	Y
F	7.5	419	Y
F	7.5	428	Y
F	7.5	479	Y
F	7.5	510	Y
F	7.5	476	Y
F	7.5	492	Y
F	7.5	454	Y
F	7.5	567	Y
F	7.5	476	Y
F	7.5	497	Y
F	7.5	460	Y
F	7.5	443	Y
F	7.5	435	Y
F	7.5	426	Y
F	7.5	476	Y
F	7.5	411	Y
M	5.5	646	
M	5.5	701	
F	3.5	381	Y
F	3.5	410	Y
F	1.5	334	
F	0.5	110	
F	0.5	144	
M	0.5	160	
F	0.5	166	
M	0.5	138	
M	0.5	152	
M	0.5	147	
M	0.5	183	
F	0.5	96	
M	0.5	208	
M	0.5	104	
M	0.5	163	
F	0.5	127	
M	0.5	136	
M	0.5	165	
M	0.5	126	
F	0.5	127	

Table S2: Composition of the first cut and second cut hay provided as a supplement to the study bison herd.

Variable (% unless otherwise noted)	First cut	Second cut
Crude Protein	9.7	17.2
Acid detergent fiber	47.9	38.3
Total digestible nutrients	48.9	59.7
Calcium	0.8	1.51
Phosphorus	0.2	0.21
Magnesium	0.21	0.32
Potassium	1.92	2.06
Sulfur	0.15	0.32
Sodium	<0.011	0.028
Zinc (mg/kg)	14	15
Iron (mg/kg)	66	61
Manganese (mg/kg)	60	56
Copper (mg/kg)	7	9

Table S3: The number of bails of first cut and second cut hay (Table S2) delivered to the bison pasture.

Date	First cut	Second cut
Nov. 17, 2017	2	2
Nov. 20, 2017		2
Nov. 22, 2017	1	2
Nov. 25, 2017		2
Nov. 27, 2017	2	2
Nov. 29, 2017		2
Dec. 1, 2017		2
Dec. 3, 2017		
Dec. 5, 2017	2	2
Dec. 8, 2017	2	2
Dec. 12, 2017		2
Dec. 15, 2017	2	2
Dec. 19, 2017	2	2
Dec. 21, 2017	2	2
Dec. 26, 2017	2	2
Dec. 28, 2017	2	2
Dec. 31, 2017	2	2
Jan. 2, 2018	2	2
Jan. 5, 2018	2	2
Jan. 8, 2018	2	2
Jan. 11, 2018	2	2
Jan. 15, 2018	2	2
Jan. 18, 2018	2	2
Jan. 22, 2018	2	2
Jan. 26, 2018		2
Jan. 27, 2018	2	
Jan. 29, 2018	1	1
Jan. 31, 2018	1	1
Feb. 3, 2018	2	2

600 **Figures**

Figure 1: The study site near Gallatin Gateway, MT (45.557, -111.229). Bison locations are mapped within the 20-meter grid here superimposed in yellow. The tower location is in cyan and game camera locations are indicated in orange. Background image: Google, Maxar Technologies and the USDA Farm Service Agency ©2018.

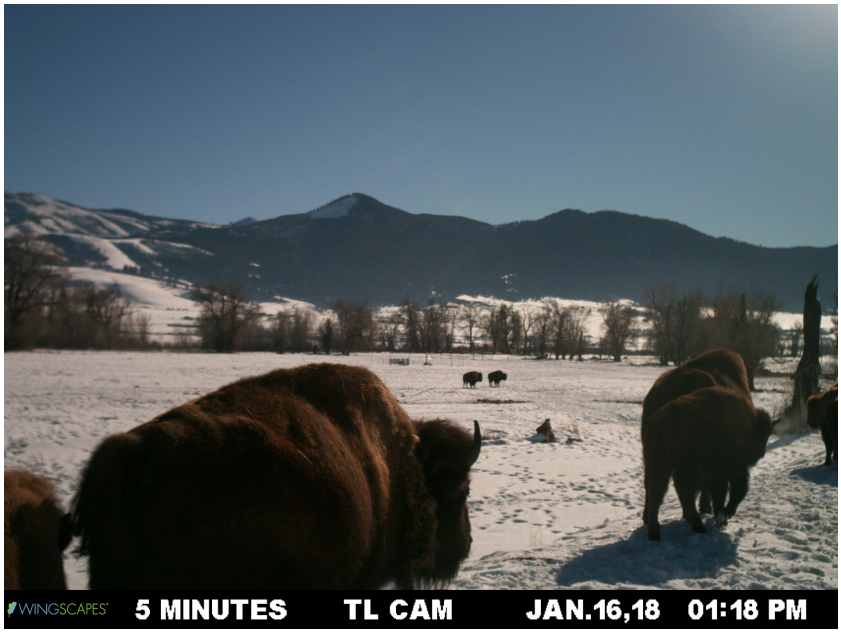

Figure 2: A sample image of bison as viewed from the south-facing time-lapse camera located to the north of the study area (Figure 1). The eddy covariance installation is visible toward the center of the study site.

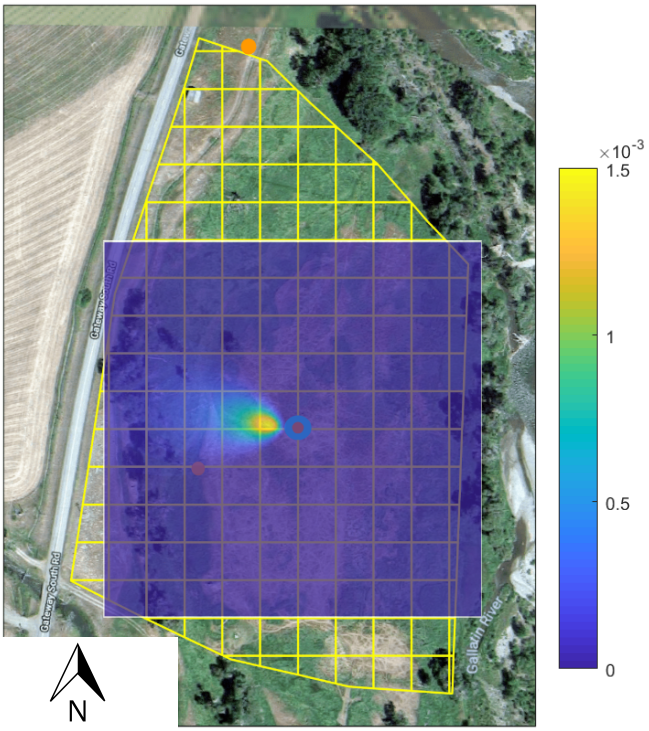

Figure 3: An eddy covariance flux footprint calculated following Hsieh et al. (2000) and Detto and Katul (2006) at 1 m resolution for a single 30-minute interval superimposed on the study field (Figure 1). The fraction of the footprint in each grid box is shown in the legend is summed for each 20 m pixel to calculate the contribution of each pixel to the total flux. Background image: Google, Maxar Technologies and the USDA Farm Service Agency ©2018.

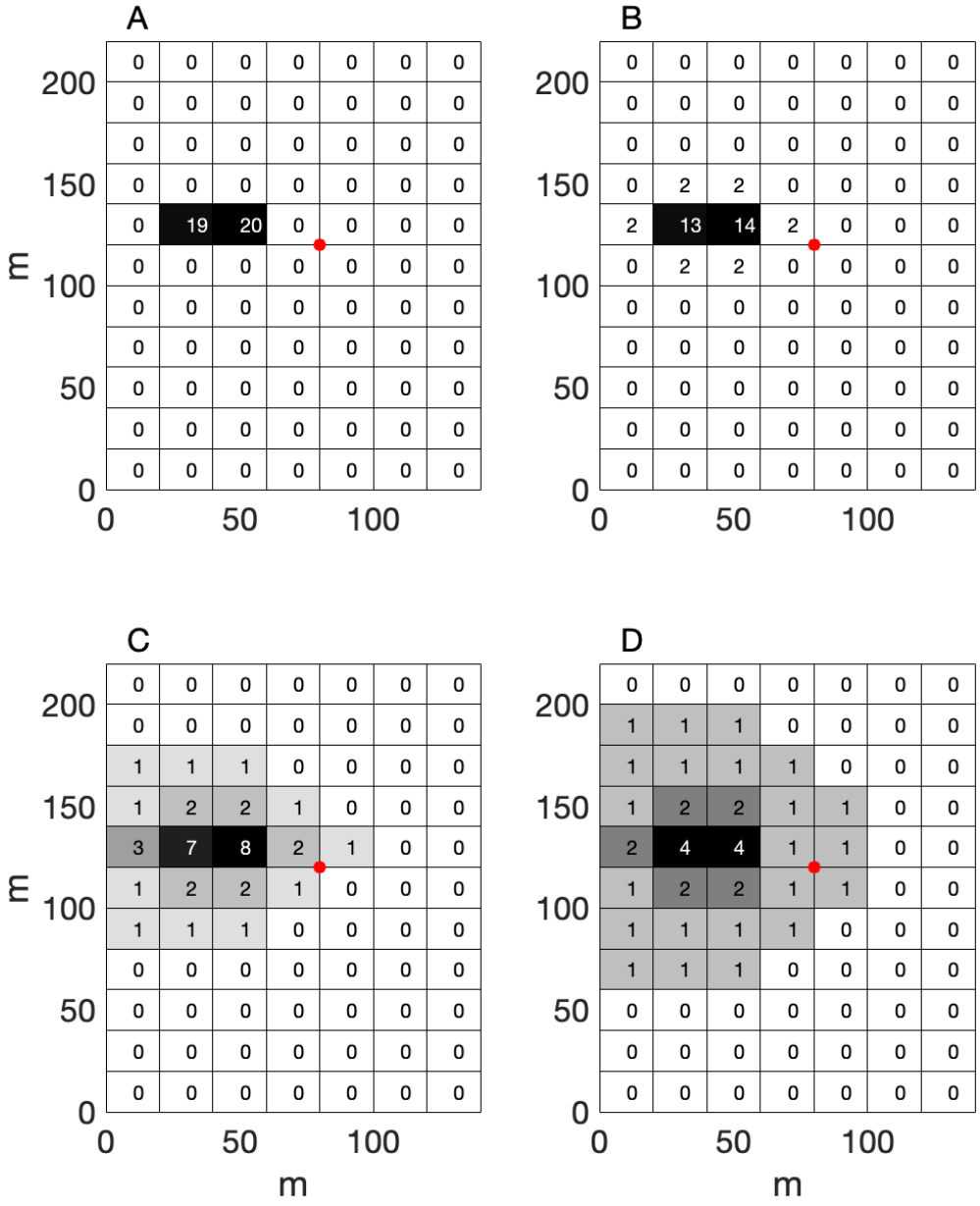

Figure 4: The number of bison observed per grid cell at 16:30 on January 11, 2017 (A) and a distributed bison location map generated using two-dimensional Tikhonov Regularization with a Lagrange multiplier of 0.1 (B), 1 (C), and 4 (D).

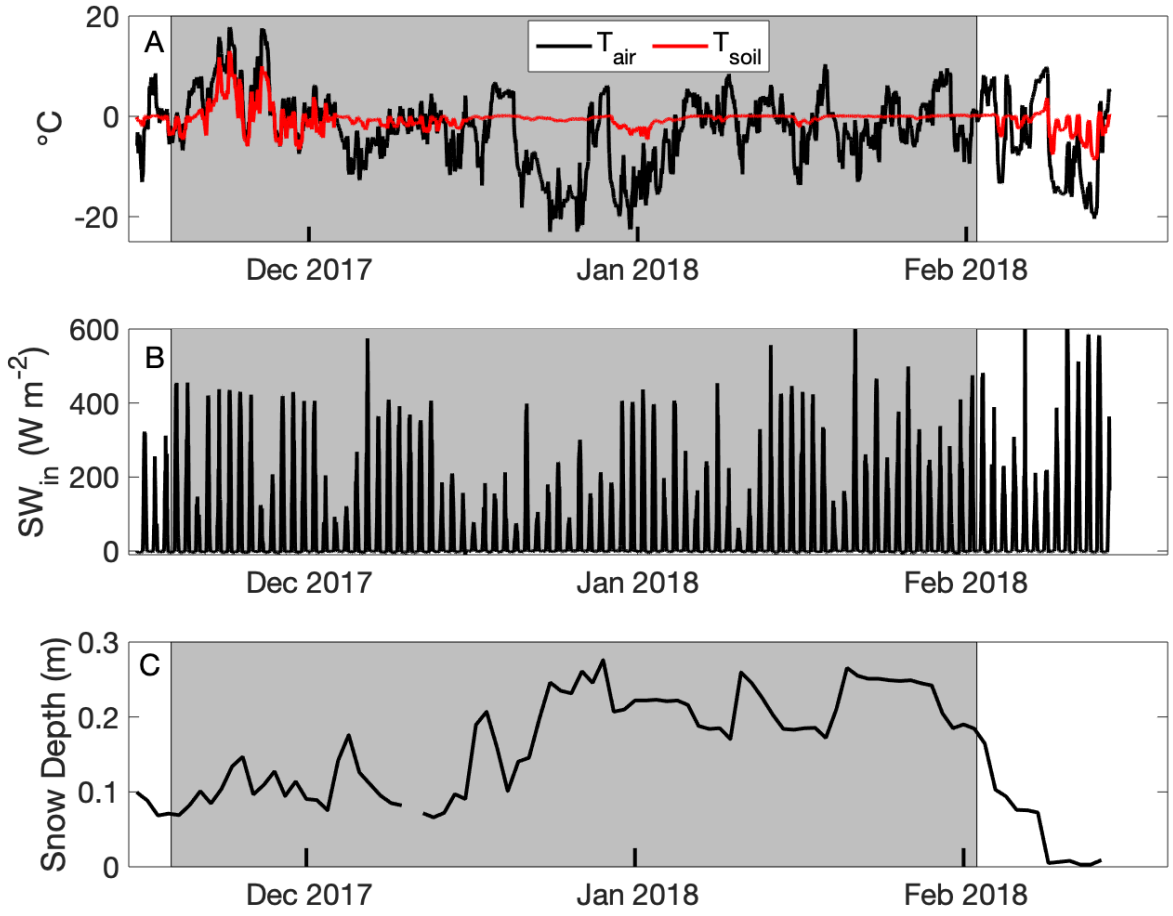

Figure 5: (A) Air (T_{air}) and soil temperature (T_{soil}), (B) incident shortwave radiation (SW_{in}), and (C) snow depth from a micrometeorological tower enclosed within an electric fence on a bison pasture near Gallatin Gateway, Montana, USA. Bison were present in the pasture during the interval bounded by the grey background.

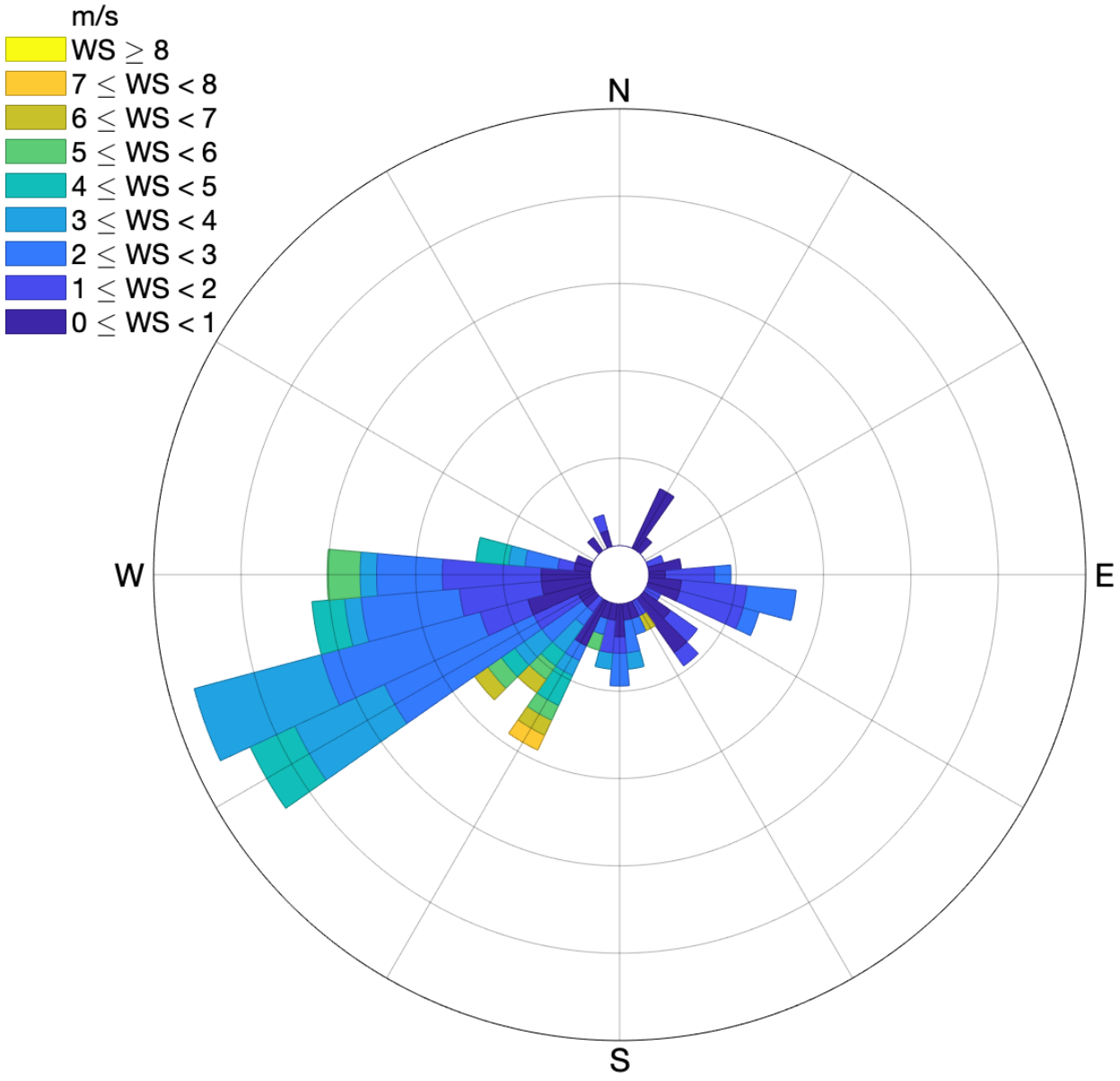

Figure 6: A wind rose following Pereira (2020) for periods when eddy covariance measurements and bison location measurements were available. WS: wind speed.

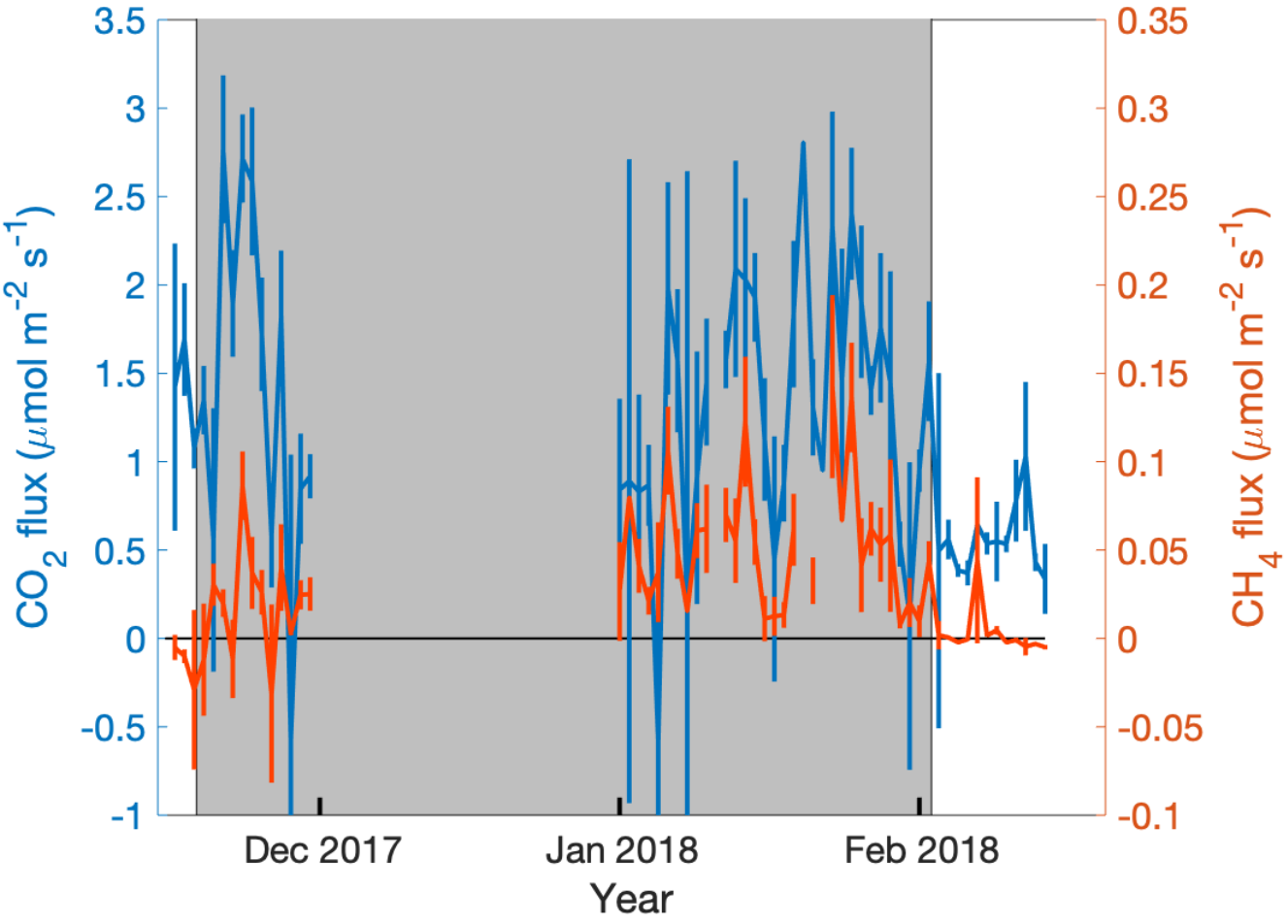

625

Figure 7: The daily mean and standard error carbon dioxide and methane fluxes with standard error during daytime hours (0700-1700) from a pasture near Gallatin Gateway, MT, USA. The gray background denotes the interval during which bison were present on the study site.

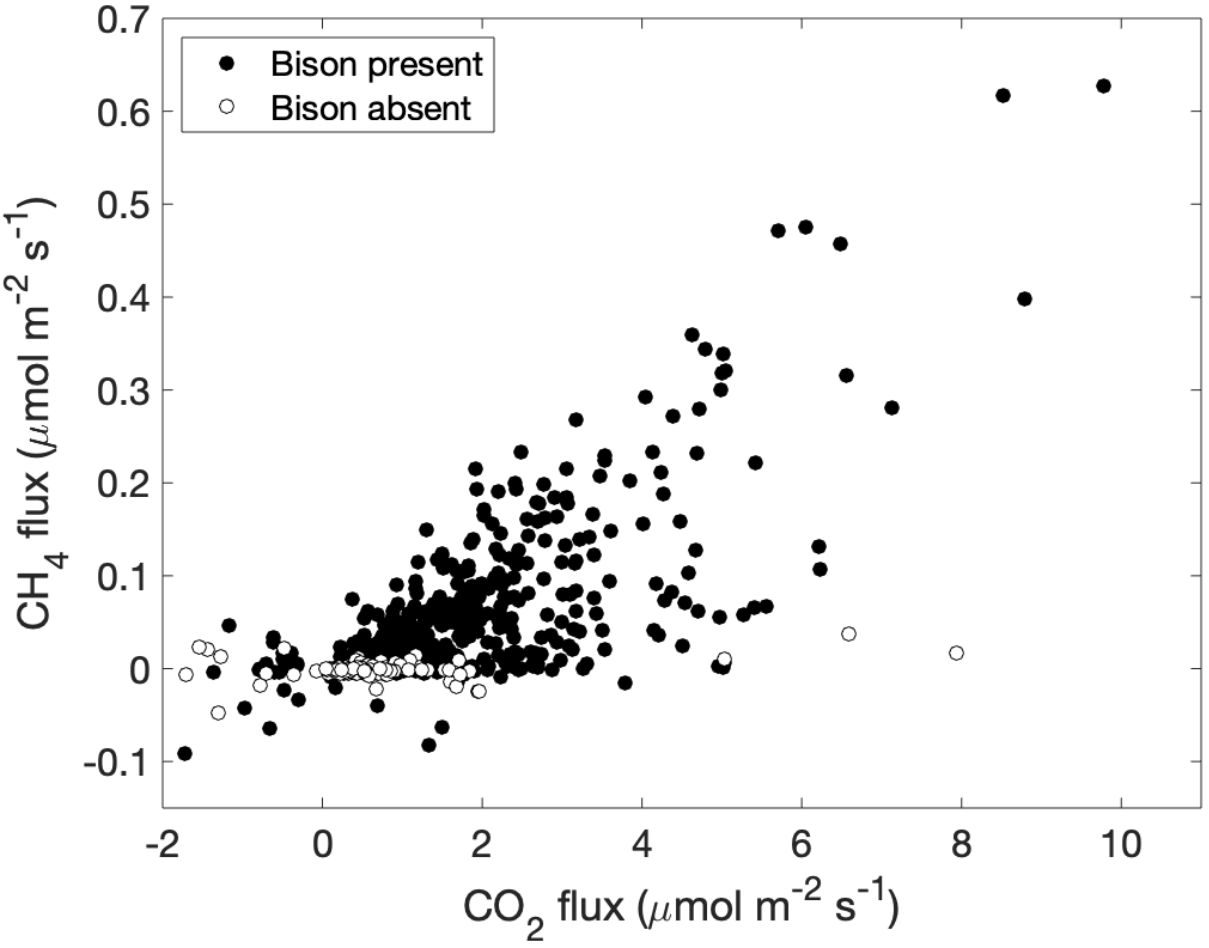

630 **Figure 8: The relationship between carbon dioxide and methane fluxes from the study pasture is shown for periods when bison were present (filled circles) and when bison were absent (open circles).**

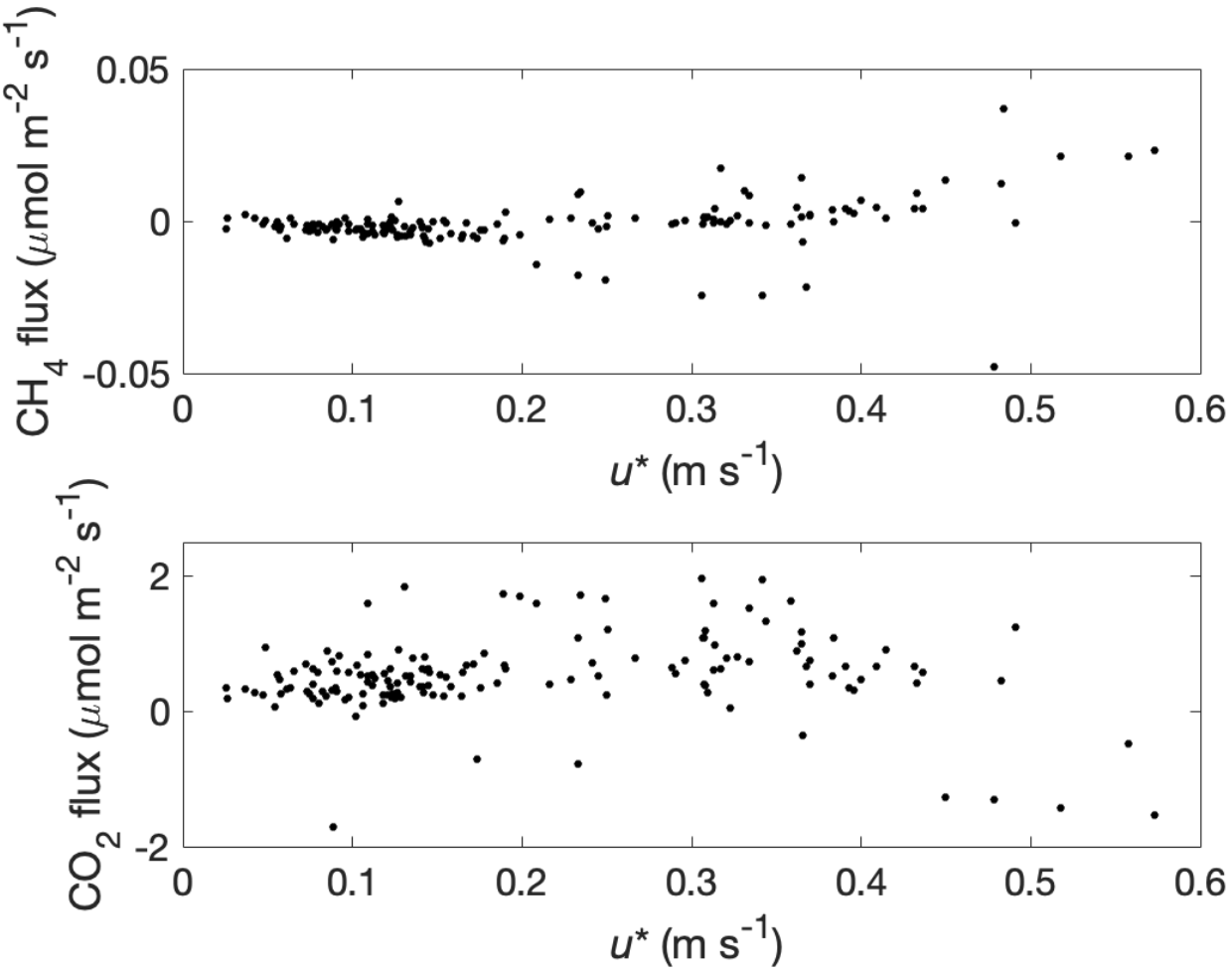

Figure 9: Methane (A) and carbon dioxide (B) fluxes as a function of friction velocity (*u) when bison were absent from the study pasture.**

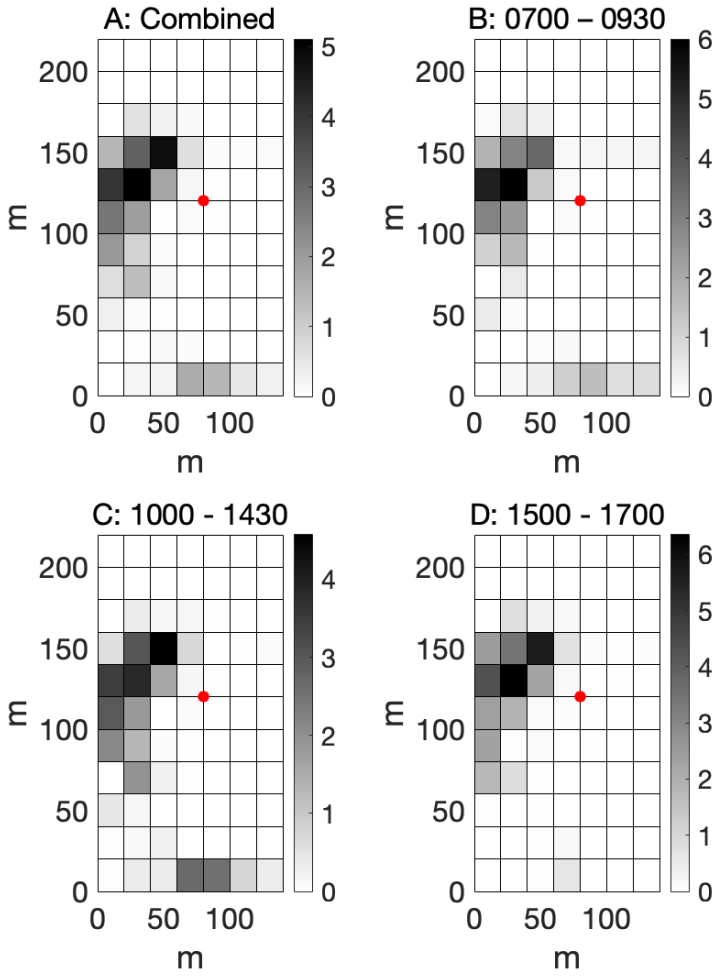

635

Figure 10: Average proportional bison density for three periods of the day. Each colored pixel represents a 20-meter grid square, red dots denote the location of the eddy covariance tower, and subplot titles refer to local time. Color denotes average proportion of bison present in each grid cell for the 39-animal herd.

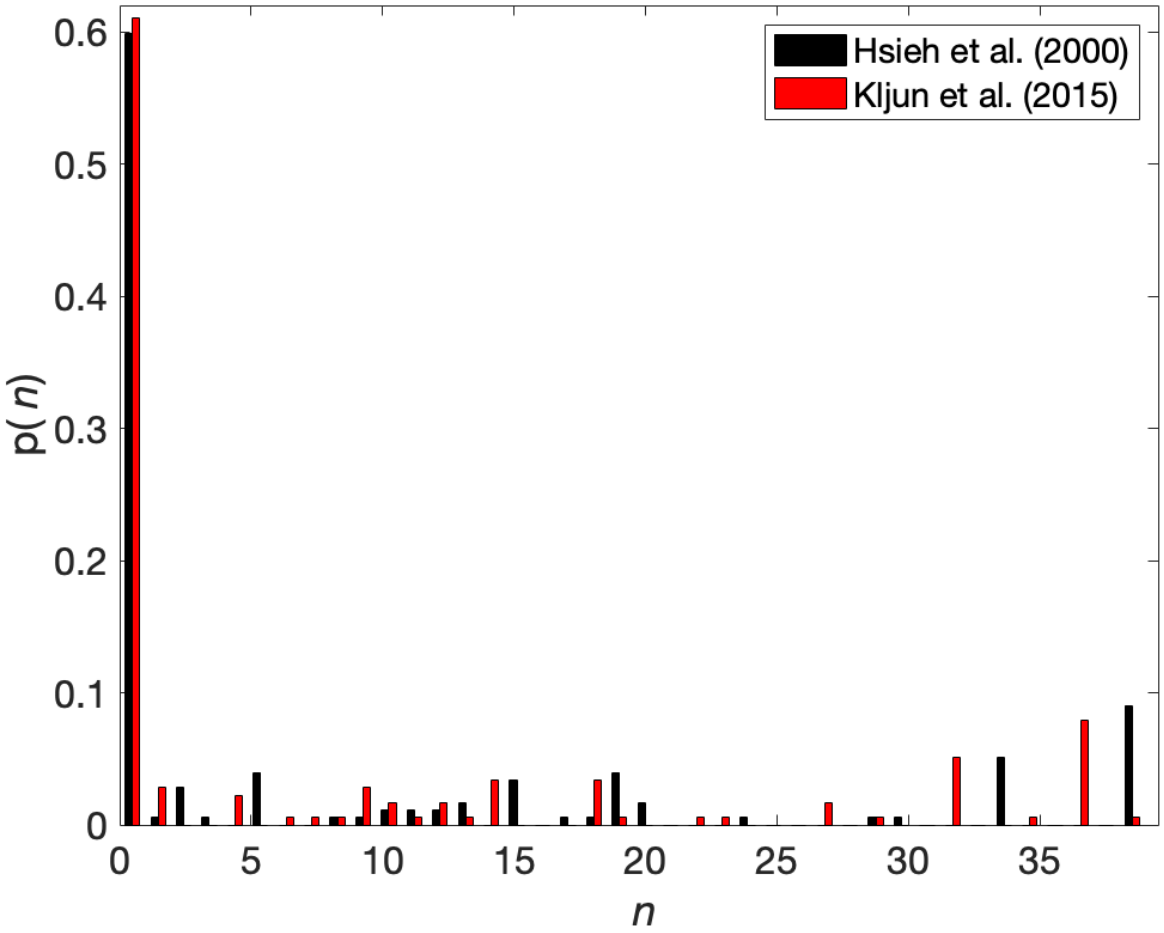

640 **Figure 11: The probability (p(n)) of the number of bison (*n*) in the 90% flux footprint for the Hsieh et al. (2000) and Kljun et al. (2015) footprint models for periods when flux measurements were made and camera imagery was available.**

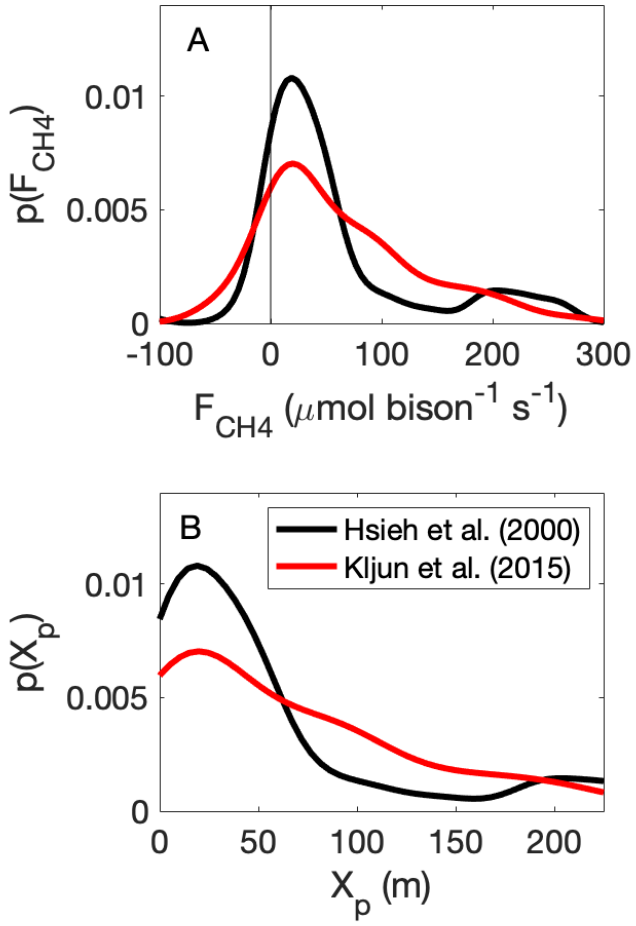

Figure 11: Kernel density estimates of the distribution (p) of (A) methane efflux (F_{CH4}) on a per-bison basis and (B) the peak (X_p)of the source-weight function for half-hourly flux footprints derived by the Hsieh et al. (2000) and Kljun et al. (2015) flux footprint models.

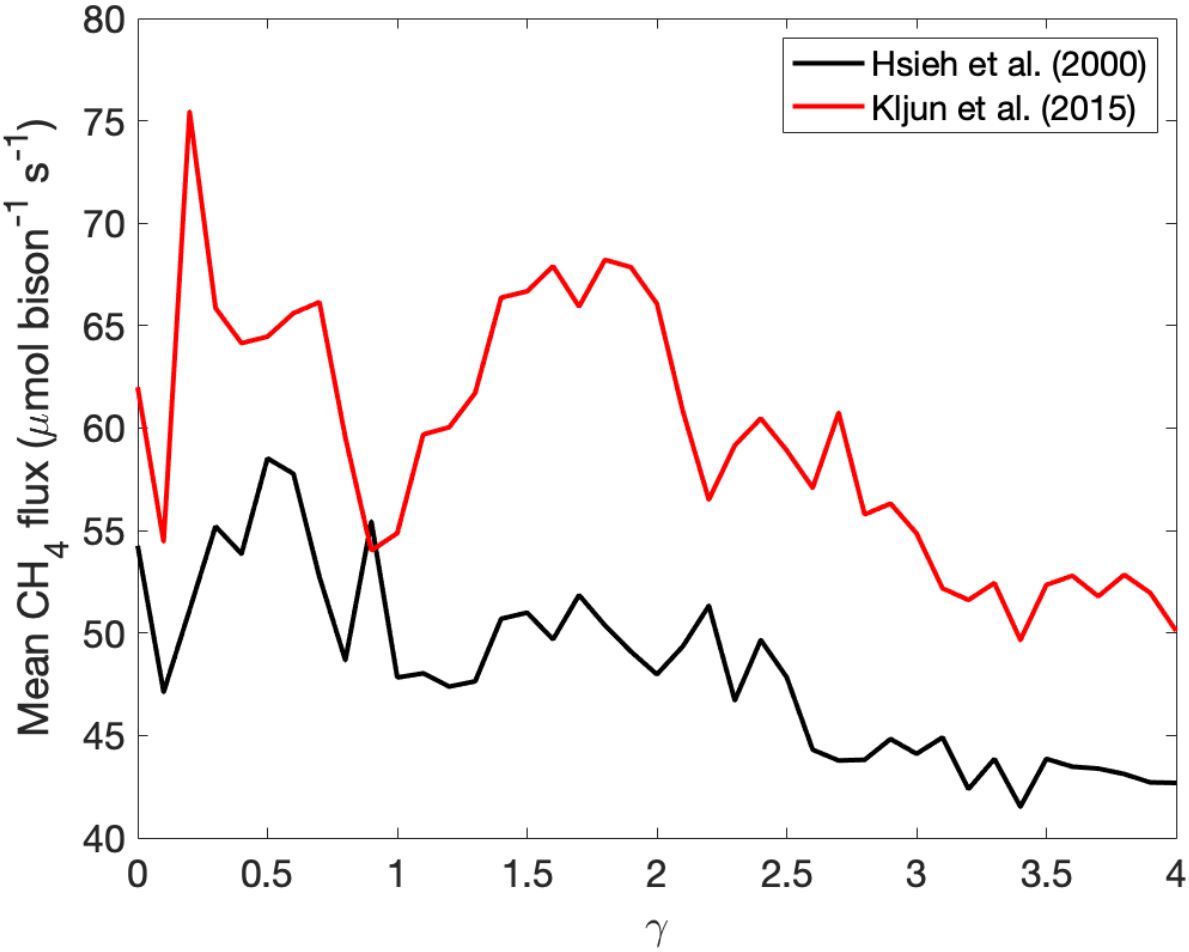

650 **Figure 12: Mean methane efflux on a per-bison basis as a function of spatial smoothing of bison location estimates using the two-dimensional Tikhonov Regularization approach described in Stoy and Quaife (2015) for different values of the Lagrange multiplier γ and the footprint models of Hsieh et al. (2000) and Kljun et al. (2015).**